ACS APPLIED MATERIALS & INTERFACES

Research Article

www.acsami.org

Charge Storage in Polymer Acid-Doped Polyaniline-Based Layer-by-Layer Electrodes

Ju-Won Jeon,[†] Josh O'Neal,[†] Lin Shao,[‡] and Jodie L. Lutkenhaus*,[†]

[†]Artie McFerrin Department of Chemical Engineering, Texas A&M University, 3122 TAMU, College Station, Texas 77843-3122, United States

[‡]Department of Chemical and Environmental Engineering, Yale University, New Haven, Connecticut 06520-8286, United States

Supporting Information

ABSTRACT: Polymeric electrodes that can achieve high doping levels and store charge reversibly are desired for electrochemical energy storage because they can potentially achieve high specific capacities and energies. One such candidate is the polyaniline:poly(2-acrylamido-2-methyl-1-propanesulfonic acid) (PANI:PAAMPSA) complex, a water-processable complex obtained via template polymerization that is known to reversibly achieve high doping levels at potentials of up to 4.5 V versus Li/Li$^+$. Here, for the first time, PANI:PAAMPSA is successfully incorporated into layer-by-layer (LbL) electrodes. This processing technique is chosen for its ability to blend species on a molecular level and its ability to conformally coat a substrate. Three different polyaniline-based LbL electrodes comprised of PANI/PAAMPSA, PANI/PANI:PAAMPSA, and linear poly(ethylenimine)/PANI:PAAMPSA are compared in terms of film growth, charge storage, and reversibility. We found that the reversibility of PANI:PAAMPSA is retained within the LbL electrodes and that the PANI/PANI:PAAMPSA electrode exhibits the best performance in terms of capacity and cycle life. These results provide general guidelines for the assembly of PANI:PAAMPSA in LbL films and also demonstrate their potential as electrochemically active components in electrodes.

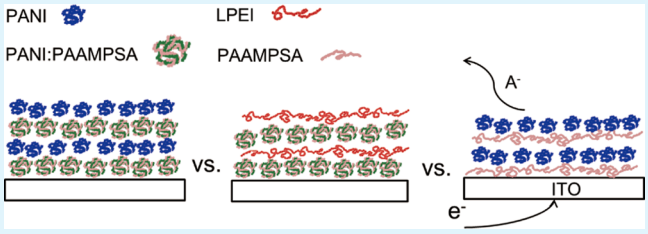

KEYWORDS: *polyaniline, poly(2-acrylamido-2-methyl-1-propanesulfonic acid), layer-by-layer assembly, electrochemical energy storage, charge storage, conducting polymer*

INTRODUCTION

Conjugated polymers, such as polypyrrole,[1,2] polythiophene,[3,4] polyacetylene,[5] and polyaniline (PANI),[6,7] have been extensively studied as electrode materials in electrochemical energy storage systems. Among them, PANI has attracted significant interest as an electrode material because of its high capacity,[8,9] good conductivity,[10] unique doping−dedoping process,[11] and ease of synthesis.[12] PANI stores charge through reduction and oxidation, or dedoping and doping, respectively. In nonaqueous electrolyte systems, polyaniline reversibly switches between leucoemeraldine base and half-doped emeraldine salt oxidation states. However, even at moderately oxidizing potentials (~3.5 V vs Li/Li$^+$), PANI gradually loses its electrochemical activity during cycling because of irreversible oxidation to pernigraniline base.[13,14] Accordingly, there is significant interest in electroactive polymers that are capable of achieving reversible charge storage at potentials of greater than 3.5 V versus Li/Li$^+$, so that higher doping levels, capacities, and energies can be achieved.[15]

One such promising candidate to emerge is the polyaniline:poly(2-acrylamido-2-methyl-1-propanesulfonic acid) (PANI:PAAMPSA) complex synthesized via template polymerization. It was recently demonstrated that PANI:PAAMPSA could reversibly store charge even at highly oxidizing potentials (~4.5 V vs Li/Li$^+$), which led to doping levels near 0.8 and an enhanced cycle life relative to that of the PANI homopolymer.[14] It was proposed that the origin of PANI:PAAMPSA's stability arose from electrostatic and hydrogen bonding interactions between protonated amines and sulfonic acid groups. This complex, previously explored for transistors,[16] electrochromic devices,[17] and sensors,[18] was formed by the polymerization of the aniline monomer in the presence of PAAMPSA. The resulting PANI:PAAMPSA product was a negatively charged, water dispersible colloid.[14,19] In a cast film, PANI:PAAMPSA exhibited a conductivity of 0.4 S/cm, which could be enhanced to 40 S/cm with dichloroacetic acid treatment.[16]

Motivated by these previous results, we hypothesized that PANI:PAAMPSA could be adapted for layer-by-layer (LbL) assembly to form thin film electrodes for energy storage. To fully leverage PANI:PAAMPSA's ability to reversibly store charge at elevated voltages, it is desirable to pursue alternative processing methods, such as LbL assembly. This technique, which is based on the alternate adsorption of oppositely charged species, is a versatile method for fabricating thin films and coatings.[20,21] Film thickness can be easily controlled, and

Received: July 14, 2013
Accepted: September 23, 2013
Published: September 23, 2013

   dx.doi.org/10.1021/am402809e | ACS Appl. Mater. Interfaces 2013, 5, 10127−10136

properties can be finely tuned by controlling pH and ionic strength.[22−24] The process is generally water-based and can proceed via dipping, spin-coating,[25] or spraying.[26] One unique feature of LbL assembly is that it can conformally deposit films onto a variety of surfaces (silicon, ITO-coated glass,[13] carbon paper,[27] etc.).

LbL assembly has been widely applied to form electrodes for electrochemical energy storage. Kim et al. fabricated LbL electrodes of multiwall carbon nanotubes (MWNTs), which resulted in a high-surface area electrode that delivered the highest energy per unit area among reported LbL electrodes (300 μW h cm^{-2} at 0.4 mW cm^{-2}).[27] Electrodes for microbatteries or electrochemical capacitors were assembled from PANI nanofibers and MWNTs, which maintained 75% of their initial capacity (160 mAh/cm^3) at 7.2 A/cm^3.[28] Interestingly, the PANI nanofiber/MWNT LbL electrodes were reversible up to 4.5 V versus Li/Li$^+$, but extensive thermal treatment was required. Intimate mixing of cathode materials such as V_2O_5 and PANI has been demonstrated via LbL assembly.[13] If PANI:PAAMPSA were to be incorporated into similar electrodes, one might be able to enhance conductivity and attain reversible charge storage at high potentials, without the need for thermal treatment.

To date, there have been no reports of PANI:PAAMPSA in LbL assemblies, so it was not immediately clear whether PANI:PAAMPSA could be assembled or processed via this technique. Earlier work with poly(3,4-ethylenedioxythiophene) (PEDOT):PSS, which is synthesized in a fashion similar to that of PANI:PAAMPSA, demonstrated its successful incorporation into an LbL assembly.[29,30] The electrochromic activity of PEDOT:PSS was retained in the LbL assembly, and good contrast between bleached and colored states was demonstrated. These results suggested that PANI:PAAMPSA, because it is structurally similar to PEDOT:PSS, might be suitable for LbL assembly; however, it was not known if PANI:PAAMPSA would retain its stability and reversible charge storage.

Here, the successful LbL assembly of PANI:PAAMPSA with complementary polycations is presented for the first time, as is the retention of its reversible charge storage. To assess the nature of charge storage, three different polyaniline-based LbL electrodes comprised of PANI/PAAMPSA, PANI/PANI:PAAMPSA, and linear poly(ethylenimine)/PANI:PAAMPSA are compared. The first system is proposed as an LbL mimic of the PANI:PAAMPSA complex, and the second is proposed as an electrode with high PANI content. The last electrode isolates the performance of PANI:PAAMPSA alone within the LbL assembly because poly(ethylenimine) is not electrochemically active. The growth and structure of the LbL electrodes are characterized using profilometry, ζ potential, UV−vis spectroscopy, Fourier transform infrared (FTIR) spectroscopy, and a quartz crystal microbalance (QCM). Charge storage is assessed using cyclic voltammetry and galvanostatic charge−discharge cycling. These results provide general guidelines for the assembly of PANI:PAAMPSA in LbL films and also demonstrate their potential as electrochemically active components in electrodes.

EXPERIMENTAL SECTION

Materials. PANI, dimethylacetamide (DMAc), hydrochloric acid, aniline, (3-aminopropyl)triethoxysilane (APTES), propylene carbonate, lithium perchlorate, and ammonium peroxydisulfate were purchased from Sigma-Aldrich. Poly(2-acrylamido-2-methyl-1-propanesulfonic acid) (PAAMPSA, 10.36 wt % in water, $M_w \sim 800$ kg/mol) was purchased from Scientific Polymer Products. Linear poly(ethylenimine) (LPEI) ($M_w \sim 25000$) was obtained from Polysciences. Indium−tin oxide (ITO)-coated glass was obtained from Delta Technologies. Lithium metal was obtained from Alfa Aesar.

Synthesis of PANI:PAAMPSA. PANI:PAAMPSA was synthesized according to previous reports.[14,31] Briefly, 5.8 g of PAAMPSA (0.028 mol) was dissolved in 375 mL of deionized water. Aniline (2.6 g, 0.028 mol) was mixed with the PAAMPSA solution and stirred for 1 h. Ammonium peroxydisulfate (5.8 g, 0.025 mol) was also dissolved in 25 mL of deionized water separately. Both aniline/PAAMPSA and ammonium peroxydisulfate solutions were purged with nitrogen. The ammonium peroxydisulfate solution was added dropwise to the aniline/PAAMPSA solution, and polymerization was conducted at 5 °C for 24 h. Then, acetone was added to precipitate the PANI:PAAMPSA, which was filtered and washed with acetone to remove unreacted monomer and oligomer. The isolated PANI:PAAMPSA colloid was dried under vacuum at room temperature overnight.

Layer-by-Layer Assembly. PANI:PAAMPSA (0.2 g) was dispersed in 400 mL of deionized water by a 10 h mild sonication. To prevent overheating during sonication, ice was added to the bath. After sonication, the pH of the PANI:PAAMPSA dispersion was adjusted to 2.5 using dilute HCl.

The PANI dispersion was prepared as described previously.[13,32] The emeraldine base form of PANI (0.2 g) was dissolved in 40 mL of DMAc, stirred for 12 h, and sonicated for 10 h. The resulting solution was then filtered through a 0.7 μm glass filter. The filtrate was slowly added to pH 3.0−3.5 deionized (DI) water (360 mL). The resulting mixture was then quickly adjusted to pH 2.5 and filtered again before being used.

For the PAAMPSA solution, PAAMPSA (0.2 g) was mixed with 400 mL of DI water. For the LPEI solution, LPEI (0.2 g) was also dissolved in 400 mL of DI water, and the pH was adjusted to 2.5. PANI/PAAMPSA, PANI/PANI:PAAMPSA, and LPEI/PANI:PAAMPSA LbL films were built onto APTES-treated, ITO-coated glass substrates. First, ITO-coated glass was sonicated sequentially in dicholoromethane, acetone, methanol, and DI water for 15 min each. After being washed, the ITO-coated glass was then stored in DI water before being used. When ready for use, the washed ITO-coated glass was then blown dry using nitrogen gas and placed in a convection oven at 50 °C. The substrates were then exposed to oxygen plasma (Harrick PDC-32G) for 5 min and then immediately immersed in 2 vol % APTES in toluene for 30 min at 75 °C.[14,33] APTES-treated substrates were washed with toluene, ethanol, and finally DI water. The substrates were then blown with nitrogen gas to remove the remaining deionized water and placed in an oven at 110 °C for 15 min.

LbL assembly was conducted using an automated slide stainer (HMS Series, Carl Zeiss, Inc.). The APTES-treated substrates were immersed in the dispersion (or solution) containing the negatively charged species (PANI:PAAMPSA or PAAMPSA) for 15 min and rinsed in three different deionized water baths for 2, 1, and 1 min. The substrates then were immersed in the dispersion (or solution) containing the positively charged species (PANI or LPEI) for 15 min, followed again by rinsing. This cycle was repeated until the desired number of layer pairs was achieved. For LbL assembly, the pH of all solutions and dispersions was adjusted to 2.5. The assembled film is denoted as (cationic species/anionic species)$_n$, where n is number of layer pairs.

Characterization. Profilometry (P-6, KLA-Tencor) was used to measure the thickness of the LbL film. Five locations per sample were measured, and the average value was taken as its thickness. UV−vis spectroscopy of the assembled films was measured using a Hitachi U-4100 spectrometer. For the measurement, bare ITO-coated glass was used as a baseline. To obtain the density and composition of each LbL film, a QCM (Inficon) was employed. A 5 MHz Ti/Au quartz crystal was washed and exposed to oxygen plasma for 5 min. Then, the bare crystal was measured as the baseline. LbL assembly was conducted on the quartz crystal as described above. Before the QCM measurement, the LbL-coated quartz crystal was dried under nitrogen for 10 min to remove the remaining water. Fourier transform infrared (FTIR)

spectroscopy was performed using a Bruker Optics spectrometer (ALPHA-P 10098-4) at 2 cm^{-1} resolution; samples were scanned 1024 times, and bare ITO-coated glass was used as a baseline. ζ potential and dynamic light scattering (DLS) measurements were taken using a Zetasizer (Nano ZS90, Malvern Instruments); for the measurement, the concentration of the dispersion was adjusted to 0.005 wt %. The electrochemical properties of the LbL films were assessed in a three-electrode cell. LbL-coated ITO-coated glass was used as the working electrode, and lithium ribbon was used as the counter and reference electrodes; 0.5 M $LiClO_4$ dissolved in propylene carbonate was used as an electrolyte. All electrochemical measurements were performed using a Solartron SI 1287 instrument at room temperature in a water-free, oxygen-free glovebox [<2 ppm each (MBraun)]. Before electrochemical tests, LbL films were placed under vacuum and then immersed in an electrolyte solution for 12 h. Prior to electrochemical experiments, LbL films were conditioned via repeated cycling. For conditioning, cyclic voltammetry (1.5−3.5 V) was performed 20 and 30 times for PANI/PAAMPSA and PANI/PANI:PAAMPSA LbL electrodes, respectively. For LPEI/PANI:PAAMPSA LbL films, cyclic voltammetry (1.5−4.5 V) was conducted 250 times as conditioning. As discussed later, these voltages were selected on the basis of the relative observed cyclability of the LbL electrodes. All voltages are reported versus Li/Li^+. Conductivity was measured using a home-built four-point probe.

RESULTS AND DISCUSSION

Three different LbL electrodes were assembled: PANI/PAAMPSA, PANI/PANI:PAAMPSA, and LPEI/PANI:PAAMPSA. The motivation was to incorporate electrochemically inactive components (PAAMPSA and LPEI) so we could isolate the individual contributions of electrochemically active components (PANI and PANI:PAAMPSA). At pH 2.5, the ζ potentials of PANI and PANI:PAAMPSA colloids were 30 and −33 mV, respectively, which indicated that both species were sufficiently charged for successful LbL assembly. As expected, the PANI:PAAMPSA colloid was negatively charged because of excess sulfonic acid groups, whereas PANI was positively charged because of protonated nitrogens along the PANI backbone. Hydrodynamic diameters of PANI and PANI:PAAMPSA were measured using DLS and were 174 and 574 nm in pH 2.5 water, respectively.

Growth profiles for each LbL system exhibited very different behavior (Figure 1a). PANI/PAAMPSA and PANI/PANI:PAAMPSA LbL films grew linearly by 5.1 and 4.8 nm per layer pair, respectively. On the other hand, the LPEI/PANI:PAAMPSA LbL films grew slowly for the first 15 bilayers and then grew rapidly after 15 bilayers (~63 nm per layer pair). This type of growth profile was similar to those previously observed for other LbL systems such as poly(ethylene oxide)/poly(acrylic acid) and poly(ethylene oxide)/poly(methacrylic acid),[34,35] in which growth proceeded regularly following an induction period during which growth is nonuniform and characterized by islandlike growth.

The roughness of each system was investigated by comparing the root-mean-square (rms) roughness measured using profilometry. For LbL films consisting of 40 layer pairs, $(LPEI/PANI:PAAMPSA)_{40}$, $(PANI/PAAMPSA)_{40}$, and $(PANI/PANI:PAAMPSA)_{40}$ LbL films had rms roughnesses of 600, 4.4, and 63.3 nm, respectively (Figure S1 of the Supporting Information). Interestingly, the rms roughness of $(LPEI/PANI:PAAMPSA)_{40}$ LbL films was similar to the hydrodynamic diameter of the PANI:PAAMPSA complex (574 nm, measured using DLS). The exceptionally rough LPEI/PANI:PAAMPSA LbL surface is possibly linked to the film's nonlinear growth and the relatively large size of

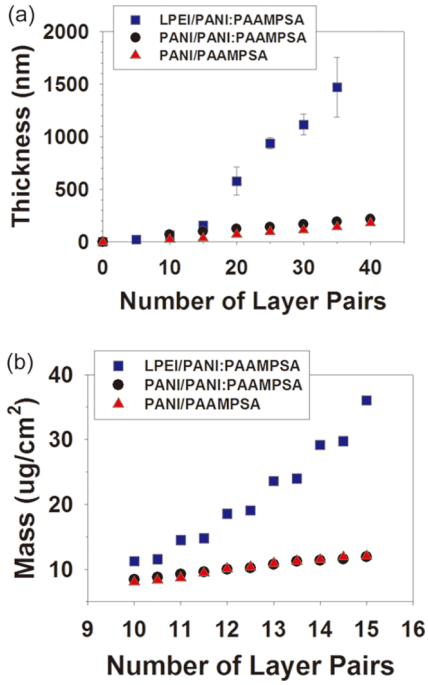

Figure 1. (a) Growth profiles and (b) adsorbed mass of LPEI/PANI:PAAMPSA, PANI/PANI:PAAMPSA, and PANI/PAAMPSA LbL films obtained using profilometry and a QCM, respectively. Error bars indicate standard deviations. In most cases, the error was smaller than the symbol.

PANI:PAAMPSA colloids. It is known that globular polyelectrolytes and colloids can engender nonlinear growth because of increasing surface roughness, which induces fractallike growth. For example, LbL assemblies of poly(hexylviologen) and PEDOT:PSS showed behavior much like what was observed here (nonlinear growth and large rms roughness that increased with number of layer pairs).[29]

The composition of the LbL films, obtained using QCM,[36,37] allowed for an accurate determination of the films' PANI content (Figure 1b, Figure S2 of the Supporting Information, and Table 1). The mass adsorbed was measured every layer

Table 1. Cationic Species, Anionic Species, and Total PANI Content of PANI/PAAMPSA, PANI/PANI:PAAMPSA, and LPEI/PANI:PAAMPSA LbL Films

	cationic species (wt %)	anionic species (wt %)	total PANI (wt %)
PANI/PAAMPSA	51	49	51
PANI/PANI:PAAMPSA	46	53	59
LPEI/PANI:PAAMPSA	8	92	23

from 10 to 15 layer pairs for dry LbL films, allowing the calculation of the weight fraction of adsorbed anionic and cationic species. For PANI/PAAMPSA and PANI/PANI:PAAMPSA LbL films, the weight ratio of cationic to anionic species was nearly 1:1. However, in the case of LPEI/PANI:PAAMPSA LbL films, PANI:PAAMPSA was the dominant species (92 wt % PANI:PAAMPSA and 8 wt % LPEI). This phenomenon might be explained by considering the fact that PANI:PAAMPSA colloids (574 nm) are much larger than LPEI polymer chains (here, $M_w \sim 25000$), so the sizes are severely mismatched. A similar mismatch in composition was observed for LbL films composed of SiO_2

and TiO_2, where the particles sizes were highly dissimilar (22 nm for SiO_2 vs 7 nm for TiO_2).[38]

To improve our understanding of the high degree of asymmetry in composition, the ratio of surface area to volume was also calculated for both PANI:PAAMPSA and LPEI. This quantity represents the area and volume over which charge is distributed. Using hydrodynamic radii of 287 nm (measured here using DLS) and 6.4 nm (from ref 39) for PANI:PAAMPSA and LPEI, respectively, R^2/R^3 could be roughly estimated to be 0.0035 and 0.16 nm^{-1}. Assuming that charge is distributed uniformly along the surface, that PANI:PAAMPSA and LPEI have equal densities, and that charge neutrality holds within the LbL film, one can roughly state that the charge on an individual PANI:PAAMPSA complex is much more diffuse than the charge on an LPEI chain. Following this reasoning, more PANI:PAAMPSA is adsorbed than LPEI, which maintains charge neutrality, leading to a film composition with a high degree of asymmetry.

Because PANI:PAAMPSA contains 25 wt % PANI,[14] the LbL films' total PANI content could also be estimated (Table 1). Here, it was assumed that PANI:PAAMPSA remains intact during the LbL assembly process because of the strong interactions between PANI and PAAMPSA.[14] Electrochemical characterization presented later supports the validity of this assumption. Of the three systems investigated, PANI/PANI:PAAMPSA LbL films contained the highest weight fraction of PANI (59 wt %), of which 78 wt % originated from PANI layers and 22 wt % originated from PANI:PAAMPSA layers.

Using data from QCM and profilometry, the density of each LbL system was estimated. Details regarding the density calculation are available in the Supporting Information. The PANI/PAAMPSA LbL film was the most dense, at 1.28 g/cm^3, followed by LPEI/PANI:PAAMPSA at 1.2 g/cm^3. PANI/PANI:PAAMPSA LbL films were the least dense, at 1.06 g/cm^3; this lower density presumably arises from the nature of the adsorbing species, where both are colloidal particles and pack less efficiently. In contrast, the other denser LbL films consisted of colloidal particles and polyelectrolytes, which perhaps packed more efficiently because of the flexibility of PAAMPSA or LPEI chains.

UV−vis spectra indicate that PANI exists as conductive emeraldine salt in each of the as-assembled LbL electrodes investigated (Figure 2). In PANI/PAAMPSA and PANI/PANI:PAAMPSA LbL systems, peaks near 310 and 420 nm were observed as well as a long absorption band (600−1200 nm). The 310 nm peak is attributed to the $\pi-\pi^*$ transition of PANI's benzenoid ring.[14,16,17,19,31,40−43] The peak at 420 nm and the long absorption band in the near-IR region are ascribed to polaron bands, which are characteristic of a conductive emeraldine salt.[16,17,42,44] The trend in absorbance at 830 nm versus the number of layer pairs (Figure 2, insets) mimicked the growth profiles obtained via profilometry. As the number of layer pairs increased, each LbL electrode investigated became a darker shade of green (Figure S3 of the Supporting Information), consistent with film growth.

In the case of LPEI/PANI:PAAMPSA LbL films, the behavior slightly deviated from that of the other two LbL systems. A maximal peak at 825 nm was observed as well as peaks at 340 and 430 nm. The red shift of the benzenoid $\pi-\pi^*$ transition peak can be ascribed to interactions between PANI:PAAMPSA and LPEI. It has been reported that electron-withdrawing groups lower the energy level of the lowest unoccupied molecular orbital (LUMO), which leads to red-shifted absorption bands.[41,45] Also, the absorbance value from 1000 to 1200 nm for LPEI/PANI:PAAMPSA LbL films significantly decreased compared to those of PANI/PAAMPSA and PANI/PANI:PAAMPSA LbL films. This decrease in absorbance suggests that PANI chains residing in the PANI:PAAMPSA colloid are more coiled than PANI chains residing in the as-synthesized PANI homopolymer.[16,17,31,46,47] This finding complements prior work, which has demonstrated that PANI chains residing within a PANI:PAAMPSA complex have an intrinsically coiled conformation.[16,17,24]

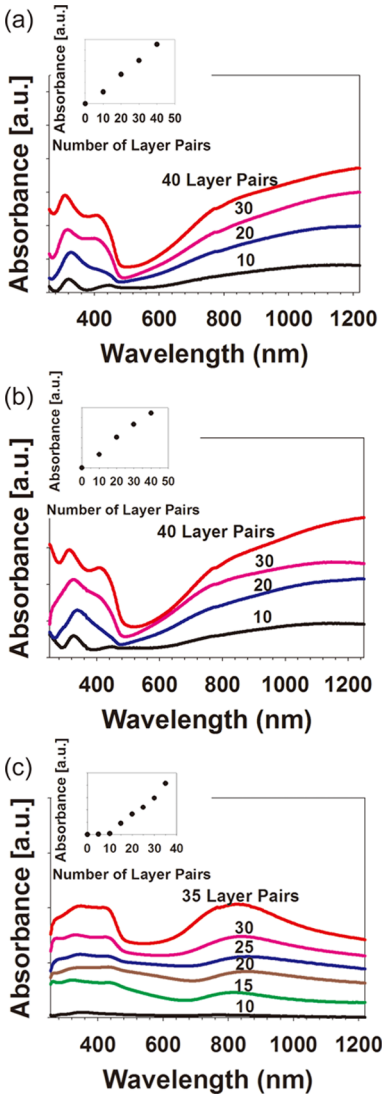

Figure 2. UV−vis spectra of (a) PANI/PAAMPSA, (b) PANI/PANI:PAAMPSA, and (c) LPEI/PANI:PAAMPSA LbL films. The insets are UV−vis absorbance intensity at 830 nm vs the number of layer pairs.

FTIR spectroscopy confirmed the chemical structure of the LbL films (Figure 3). PANI/PAAMPSA and PANI/PANI:PAAMPSA FTIR spectra were similar to spectra of the polyaniline homopolymer.[14,48−51] Peaks at 1585 and 1480 cm^{-1} are ascribed to quinoid and benzenoid ring structures, respectively.[48,50,51] Several peaks at 1648, 1038, and 625 cm^{-1} are attributed to S═O, SO_3H, and N−H (amide), respectively, originating from PAAMPSA.[14,44] In addition, the peak around 1155 cm^{-1} indicates the presence of hydronium sulfonate

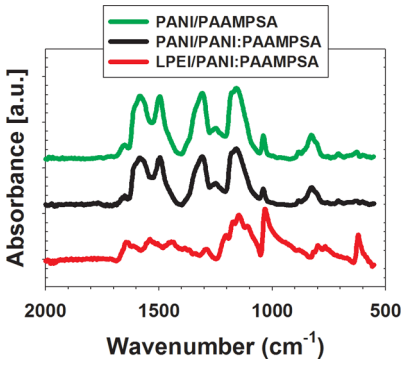

Figure 3. FTIR spectra of PANI/PAAMPSA, PANI/PANI:PAAMPSA, and LPEI/PANI:PAAMPSA LbL films.

salts.[52] In the case of LPEI/PANI:PAAMPSA LbL films, FTIR spectra were very similar to spectra from the other two systems but with a notable exception. Peaks associated with benzenoid (1440 cm^{-1}) and quinoid (1540 cm^{-1}) rings shifted to lower wavenumbers compared to those of the other systems, which may be explained by interactions between PANI:PAAMPSA and LPEI.[53,54]

Our prior work with PANI:PAAMPSA has shown that charge can be reversibly stored up to 4.5 V versus Li/Li^+.[14] By extension, the PANI/PAAMPSA LbL film, representing the LbL analogue of the PANI:PAAMPSA complex obtained via template polymerization, could presumably possess similar exceptional reversibility at high voltages. To test this hypothesis, cyclic voltammetry was conducted for 200 nm thick $(PANI/PAAMPSA)_{40}$, $(PANI/PANI:PAAMPSA)_{40}$, and $(LPEI/PANI:PAAMPSA)_{16}$ LbL films in a three-electrode cell (Figure 4). Of the three electrodes investigated, only the LPEI/PANI:PAAMPSA LbL electrode demonstrated reversibility when cycled between 1.5 and 4.5 V versus Li/Li^+ (Figure 4e). For the other two systems, the current decreased as the electrode was cycled (Figure 4a,c), indicating a decrease in the electrochemical activity of electrodes likely attributed to the irreversible oxidation of emeraldine salt to pernigraniline base.[14] On the other hand, for LPEI/PANI:PAAMPSA LbL films, the current continuously increased up to 250 cycles and then stabilized (Figure 4e). This phenomenon is termed conditioning, which is discussed later. However, the current (per mass of PANI) was much smaller than those of PANI/PAAMPSA and PANI/PANI:PAAMPSA LbL electrodes. This fact suggests that the electrochemical activity of LPEI/PANI:PAAMPSA LbL films was much lower than those of PANI/PAAMPSA and PANI/PANI:PAAMPSA LbL films. We attribute the low electrochemical activity of LPEI/PANI:PAAMPSA LbL electrodes to its low PANI content, which perhaps leads to difficulty in forming electronically percolative domains. This idea is supported by the fact that a four-point probe was unable to measure the conductivity of an LPEI/PANI:PAAMPSA LbL electrode. In contrast, the conductivities of PANI/PANI:PAAMPSA and PANI/PAAMPSA LbL electrodes were measurable, having values of 0.067 and 8.4×10^{-5} S/cm, respectively.

These findings show that reversible charge storage at high voltages is maintained for the PANI:PAAMPSA complex within an LbL film. On the other hand, the PANI/PAAMPSA LbL film, which was intended to mimic the PANI:PAAMPSA complex, did not possess good reversibility. We can infer from these results that reversibility arises from the structure of the complex itself and not the LbL assembly. Within the PANI:PAAMPSA complex, PANI is intimately intertwined with PAAMPSA as a result of template polymerization. Within the PANI/PAAMPSA LbL assembly, PANI exists as a colloidal particle rather than an individual polyelectrolyte chain and there are fewer PANI−PAAMPSA interactions than in the analogous complex.

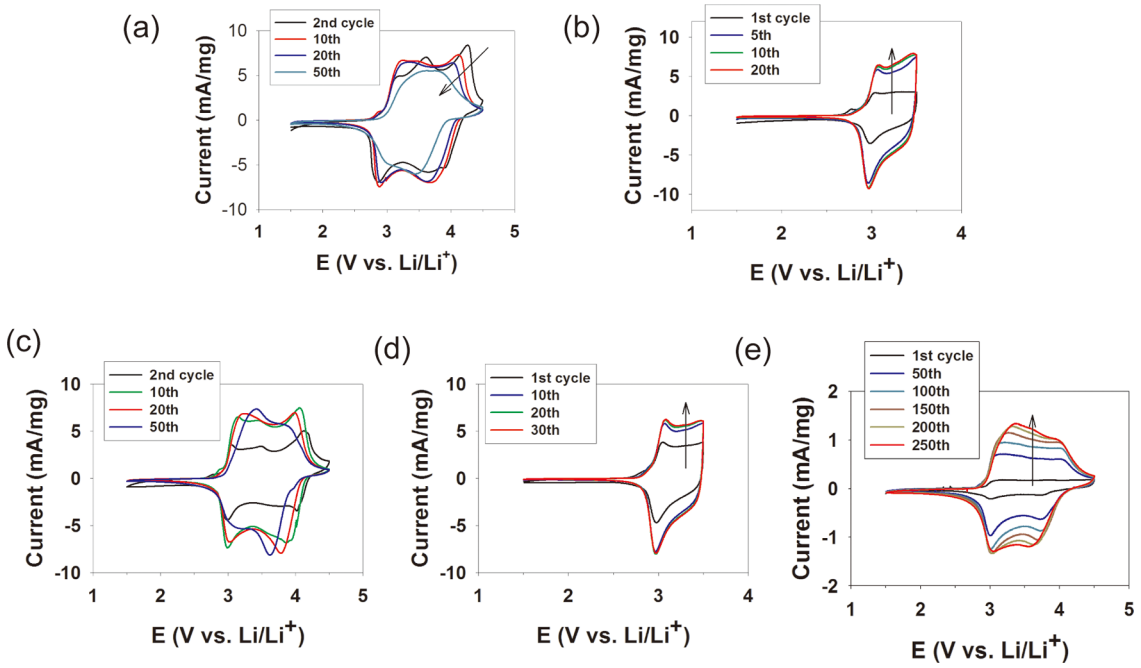

Figure 4. Cyclic voltammograms of a PANI/PAAMPSA LbL electrode (a) from 1.5 to 4.5 V and (b) from 1.5 to 3.5 V, a PANI/PANI:PAAMPSA LbL electrode (c) from 1.5 to 4.5 V and (d) from 1.5 to 3.5 V, and an LPEI/PANI:PAAMPSA LbL electrode (e) from 1.5 to 4.5 V. All films were ~200 nm thick. The current was reported per milligram of PANI, and the scan rate was 10 mV/s.

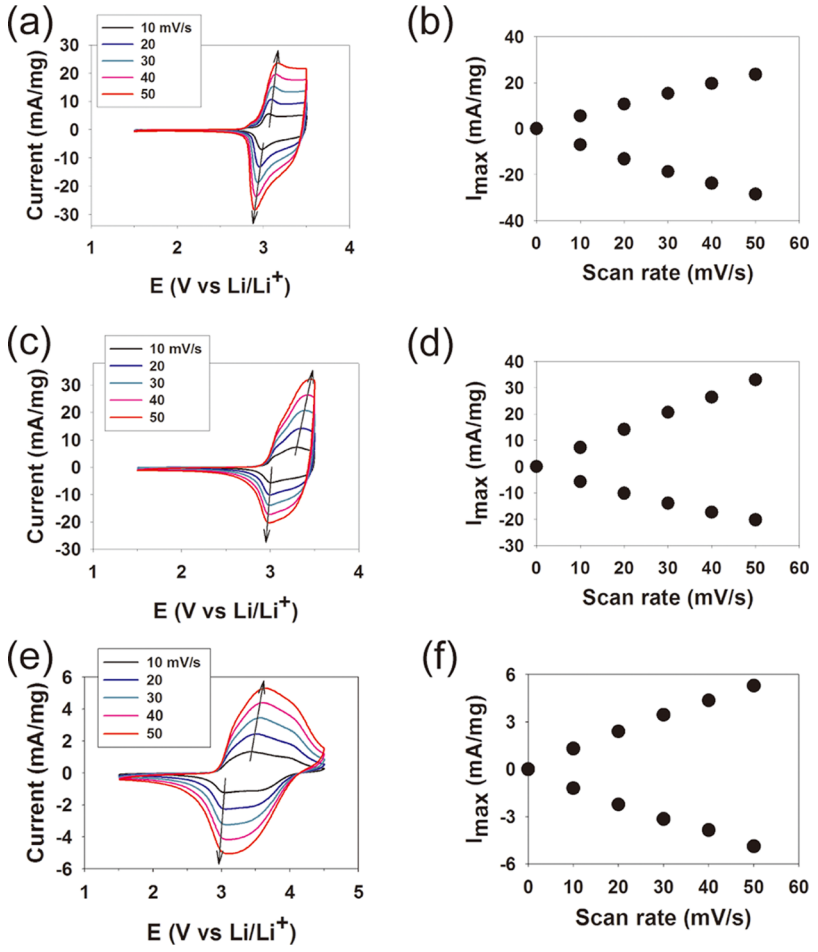

Figure 5. Cyclic voltammograms of (a) $(PANI/PAAMPSA)_{40}$, (c) $(PANI/PANI:PAAMPSA)_{40}$, and (e) $(LPEI/PANI:PAAMPSA)_{16}$ LbL electrodes. (b, d, and f) Plots of the first peak's current vs scan rate using data from cyclic voltammograms (a, c, and e, respectively). The current was reported per milligram of PANI. Each of the electrodes had been conditioned as described in the Experimental Section.

When the upper voltage was decreased from 4.5 to 3.5 V versus Li/Li^+, PANI/PAAMPSA and PANI/PANI:PAAMPSA LbL electrodes exhibited a greater degree of reversibility and stability (Figure 4b,d). For the former, the current increased and then saturated after 20 cycles, and for the latter, 30 cycles were required to reach saturation. The gradual increase in current with cycling is termed "conditioning" and has been observed on several other occasions.[13,14,55−58] According to those reports, this phenomenon results from (1) the displacement of hydronium ions (associated with sulfonic acid groups) with lithium ions and solvent[14,55−57] and/or (2) gradual penetration of the electrolyte into the electrode during the cycle.[13,58]

Having identified the optimal operating voltages and conditioning treatment for each LbL electrode, we conducted cyclic voltammetry to determine the types of electrochemical reactions present and whether they are reaction- or diffusion-controlled (Figure 5). For PANI/PAAMPSA and PANI/PANI:PAAMPSA LbL films, the maximal cutoff voltage was 3.5 V because rapid degradation was observed at higher voltages for those LbL films. For LPEI/PANI:PAAMPSA LbL films, the maximal voltage was 4.5 V versus Li/Li^+. A pair of redox peaks associated with the conversion of fully reduced leucoemeraldine base to emeraldine salt around 3 V consistently appeared for all systems. From 3 to 3.5 V, a plateau region, arising from continuous faradaic charge transfer, was also observed.[14,59] In the case of LPEI/PANI:PAAMPSA LbL films, a pair of redox peaks at 3.8 V appeared, which was assigned to the conversion of emeraldine salt to fully oxidized pernigraniline salt.[14] Plots of the maximal current versus the scan rate displayed a linear relationship, which was indicative of a surface-confined redox process.[13,60] This finding was reasonable considering that the electrodes tested in this study were approximately 200 nm thick.

The capacity and cycle life were assessed for each type of conditioned LbL electrode at various C rates using galvanostatic charging and discharging within the previously determined voltage windows (Figure 6 and Table 2). The C rate was calculated as the current required to discharge the theoretical capacity of the electrode in 1 h, represented as 1 C; a C rate of 5 C represents discharge in $^1/_5$ h and so forth. Both PANI/PAAMPSA and PANI/PANI:PAAMPSA LbL electrodes stored far more energy than the LPEI/PANI:PAAMPSA electrode on a per gram of polyaniline basis. The former two electrodes' capacity declined by 23−25% as the discharge rate increased from 1 to 50 C, and the later electrode's capacity declined by 38%.

When compared against polyaniline's theoretical capacity, the differences in charge storage among the electrodes become even more apparent. For cycling between 1.5 and 3.5 V, as was done for PANI/PAAMPSA and PANI/PANI:PAAMPSA LbL electrodes, PANI switches between leucoemeraldine base and

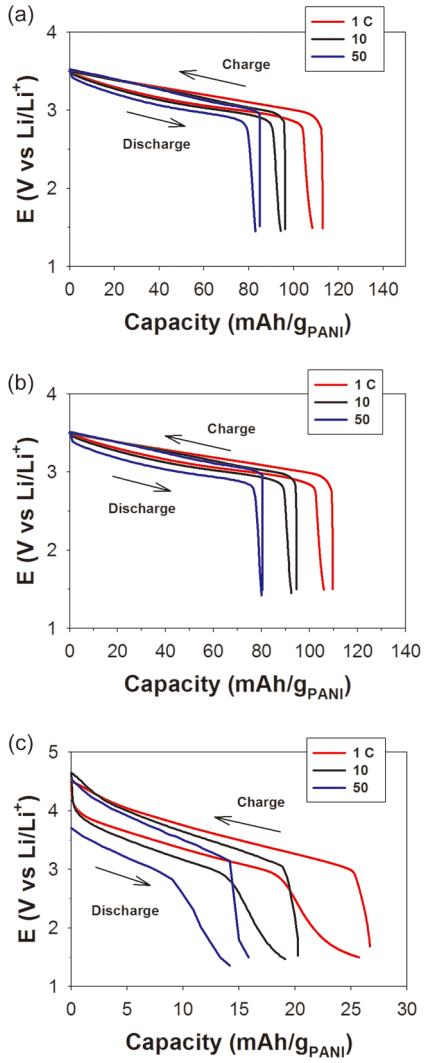

Figure 6. Galvanostatic charging and discharging of (a) PANI/PAAMPSA, (b) PANI/PANI:PAAMPSA, and (c) LPEI/PANI:PAAMPSA LbL electrodes. The capacity is based on the mass of PANI in the electrode. Each of the electrodes had been conditioned as described in the Experimental Section.

Table 2. Capacities (mAh/g of PANI) of PANI/PAAMPSA, PANI/PANI:PAAMPSA, and LPEI/PANI:PAAMPSA LbL Films at Different C Rates

	1 C	2 C	5 C	10 C	20 C	50 C
PANI/PAAMPSA	109	104	99	94	89	84
PANI/PANI:PAAMPSA	106	102	97	92	87	80
LPEI/PANI:PAAMPSA	26	23	21	19	18	16

emeraldine salt forms (theoretical capacity of 147 mAh/g of PANI);[14] between 1.5 and 4.5 V, as was done for LPEI/PANI:PAAMPSA LbL electrodes, PANI switches between leucoemeraldine base and pernigraniline salt forms (theoretical capacity of 294 mAh/g of PANI).[14] At low C rates, both PANI/PAAMPSA and PANI/PANI:PAAMPSA LbL electrodes have capacities slightly above 100 mAh/g of PANI, or two-thirds of their theoretical capacity. In comparison, LPEI/PANI:PAAMPSA LbL electrodes had a capacity of 26 mAh/g of PANI, or less than one-tenth of its theoretical capacity. This low capacity is most likely a result of the electrode's low conductivity.

Galvanostatic cycling at a rate of 10 C between voltages of 1.5 and 3.5 V for PANI/PAAMPSA and PANI/PANI:PAAMPSA and 1.5 and 4.5 V for LPEI/PANI:PAAMPSA LbL electrodes was performed to characterize each system's cyclability. Panels a and b of Figure 7 show that PANI/

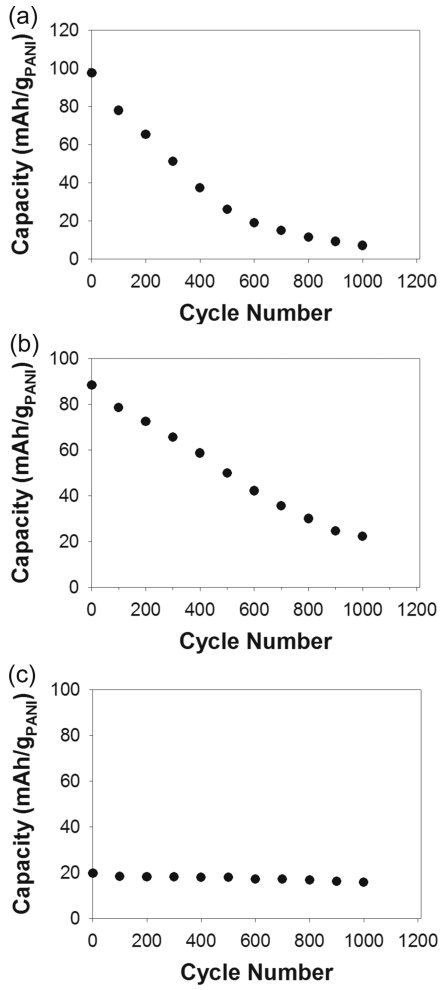

Figure 7. Cycling tests of (a) PANI/PAAMPSA, (b) PANI/PANI:PAAMPSA, and (c) LPEI/PANI:PAAMPSA LbL electrodes. Electrodes used to gather the data plotted in panels a and b were cycled between 1.5 and 3.5 V, and the electrode used to gather the data plotted in panel c was cycled between 1.5 and 4.5 V vs Li/Li^+ at a rate of 10 C. Capacity is reported on a basis of the mass of PANI in the electrode. Each of the electrodes had been conditioned as described in the Experimental Section.

PAAMPSA and PANI/PANI:PAAMPSA LbL electrodes have high initial capacities but poor cycle lives. The initial capacity of the PANI/PAAMPSA LbL electrode was 97 mAh/g of PANI (Figure 7a), which gradually declined with continued cycling. Approximately half of the initial capacity was lost after 300 cycles, and then after 1000 cycles, the capacity of the PANI/PAAMPSA LbL electrode was around 7 mAh/g of PANI. Similarly, the initial capacity of PANI/PANI:PAAMPSA LbL films was 88 mAh/g, and then after 550 cycles, its capacity decreased by half (Figure 7b). After 1000 cycles, only 20 mAh/g of PANI of capacity was retained.

We had initially hypothesized that PANI/PAAMPSA LbL electrodes would possess reversibility on par with PANI:PAAMPSA complex, but galvanostatic cycling (Figure 7a)

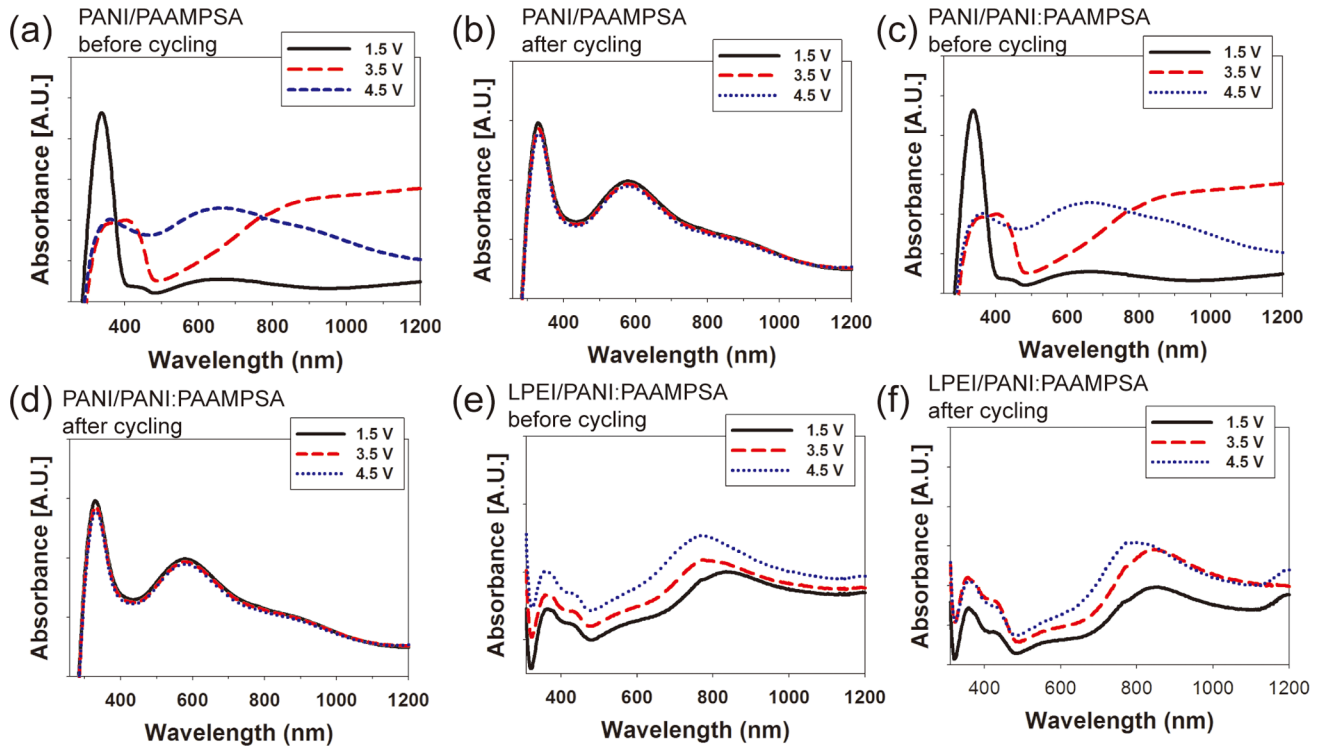

Figure 8. UV−vis spectra of PANI/PAAMPSA LbL electrodes (a) before and (b) after cycling, PANI/PANI:PAAMPSA LbL electrodes (c) before and (d) after cycling, and LPEI/PANI:PAAMPSA LbL electrodes (e) before and (f) after cycling. All electrodes were cycled from 1.5 to 4.5 V at a rate of 10 C.

clearly disproves this hypothesis. The fact that the capacity of PANI/PAAMPSA LbL electrodes declined, even under moderate potentials of 1.5 to 3.5 V, suggests that PANI/PAAMPSA LbL electrodes are not as intimately mixed as the PANI:PAAMPSA complex obtained via template polymerization. Results from cyclic voltammetry also support this idea, Figure 5. PANI/PANI:PAAMPSA LbL electrodes present an intermediate case (Figure 7b), where the capacity declines more rapidly than LPEI/PANI:PAAMPSA (Figure 7c) but less so than PANI/PAAMPSA LbL electrodes. It can be inferred from these results that PANI:PAAMPSA sustains its electrochemical activity while PANI degrades with repeated cycling.

On the other hand, the LPEI/PANI:PAAMPSA LbL electrode was the most reversible and bore the longest cycle life, albeit with lowest capacity (20 mAh/g of PANI) (Figure 7c). Because PANI:PAAMPSA's reversibility at high potentials was retained within LbL assemblies, we can conclude that the interactions between PANI and PAAMPSA were maintained and that LPEI did not significantly disrupt the PANI:PAAMPSA structure.[14] Although the LPEI/PANI:PAAMPSA conductivity was quite low, we attribute the low conductivity to LPEI, which perhaps formed a barrier to charge transport from complex to complex or layer to layer. On the other hand, the fact that a PANI/PANI:PAAMPSA LbL electrode was conductive suggests that PANI:PAAMPSA could maintain a percolative network and would, therefore, be a suitable additive for enhancing conductivity in electroactive LbL assemblies or composites.

Previously, we have shown via UV−vis spectroscopy and density functional theory modeling that PANI and PANI:PAAMPSA convert to pernigraniline base and pernigraniline salt, respectively, following repeated cycling up to 4.5 V under nonaqueous conditions.[14] Reasonably, UV−vis spectra of the three LbL systems can also be used to elucidate PANI's oxidation state as a basis for each system's stability or instability. UV−vis spectra were recorded after the electrode was held at a given potential (1.5, 3.5, and 4.5 V) before and after cycling between 1.5 and 4.5 V (Figure 8).

Before cycling, PANI/PAAMPSA and PANI/PANI:PAAMPSA UV−vis spectra were similar to each other (Figure 8a,c). At 1.5 V, an absorbance peak at 335 nm ($\pi-\pi^*$ transition) was characteristic of leucoemeraldine base.[13,43] At 3.5 V, an additional peak appeared at 420 nm as well as a long absorption band (600−1200 nm), which was typical of conductive emeraldine salt.[43,44] At 4.5 V, a broad peak appeared at 660 nm, which was the typical characteristic of pernigraniline salt.[61,62] However, after 1000 cycles (Figure 8b,d), both PANI/PAAMPSA and PANI/PANI:PAAMPSA LbL electrodes converted to pernigraniline base (peak maximum of 580 nm), regardless of the voltage applied. The fact that the UV−vis spectra remained unchanged regardless of voltage after cycling indicated that the formation of pernigraniline base was irreversible.[13,14] Conversely, LPEI/PANI:PAAMPSA LbL films exhibited spectra characteristic of emeraldine salt regardless of the applied potential both before and after cycling. The lack of clear electrochromic switching associated with the LPEI/PANI:PAAMPSA LbL film was another indication of its low electrochemical activity.

On the other hand, the good electrochromic contrast shown in PANI/PAAMPSA and PANI/PANI:PAAMPSA LbL films was apparent to the naked eye, where the film readily switched between green and transparent states at 3.5 and 1.5 V, respectively. The electrochromic behavior suggests that these films could be further explored for smart windows to control the wavelength of light absorbed or transmitted.

CONCLUSION

Three different polyaniline-based LbL electrodes (PANI/PAAMPSA, PANI/PANI:PAAMPSA, and LPEI/PANI:PAAMPSA) were successfully constructed for the first time. The nature of charge storage in each system was investigated and compared. The PANI:PAAMPSA complex maintained its ability to reversibly store charge (up to 4.5 V vs Li/Li^+) within the LPEI/PANI:PAAMPSA LbL assembly, which leads to high cyclability. After 1000 cycles between 1.5 and 4.5 V, no significant decrease in capacity was observed. In contrast, PANI/PAAMPSA and PANI/PANI:PAAMPSA LbL electrodes had larger initial capacities (97 mAh/g of PANI) because of their higher PANI content, but these same electrodes suffered from poor cyclability attributed to the irreversible formation of pernigraniline base. Also, the electrochemical reversibility of the PANI:PAAMPSA complex appears to be unique to the method of its synthesis, considering that an analogous LbL assembly of PANI and PAAMPSA was unable to emulate a similar reversibility.

This work has provided general guidelines for the incorporation of PANI:PAAMPSA into LbL assemblies, and it will now be possible to combine PANI:PAAMPSA with other active electrode materials via LbL assembly in the future. Furthermore, PANI:PAAMPSA is a promising candidate for LbL electrodes because it is both conductive and electrochemically active. An example of one such future application could be LbL hybrid electrodes containing nonconductive transition metal oxides.

ASSOCIATED CONTENT

Supporting Information

Root-mean-square roughness, growth profiles as measured via a QCM, and digital images of PANI/PAAMPSA, PANI/PANI:PAAMPSA, and LPEI/PANI:PAAMPSA LbL films with an increasing number of layer pairs. This material is available free of charge via the Internet at http://pubs.acs.org.

AUTHOR INFORMATION

Corresponding Author

*E-mail: jodie.lutkenhaus@che.tamu.edu.

Notes

The authors declare no competing financial interest.

ACKNOWLEDGMENTS

This work was supported in part by the Welch Foundation (Grant A-1766) and the Air Force Office of Sponsored Research (Grant FA9550-13-1-0147). We thank Dr. N. S. Zacharia for the profilometer and the FTIR spectrometer and Dr. M. Akbulut for ζ potential and DLS access. We thank Dr. J. Grunlan for assistance with conductivity measurements. We also thank the TAMU Materials Characterization Facility.

REFERENCES

(1) Jurewicz, K.; Delpeux, S.; Bertagna, V.; Beguin, F.; Frackowiak, E. *Chem. Phys. Lett.* **2001**, *347*, 36−40.
(2) Song, H. K.; Palmore, G. T. R. *Adv. Mater.* **2006**, *18*, 1764.
(3) Laforgue, A.; Simon, P.; Sarrazin, C.; Fauvarque, J. F. *J. Power Sources* **1999**, *80*, 142−148.
(4) Snook, G. A.; Kao, P.; Best, A. S. *J. Power Sources* **2011**, *196*, 1−12.
(5) Macinnes, D.; Druy, M. A.; Nigrey, P. J.; Nairns, D. P.; Macdiarmid, A. G.; Heeger, A. J. *J. Chem. Soc., Chem. Commun.* **1981**, 317−319.
(6) Fusalba, F.; Gouerec, P.; Villers, D.; Belanger, D. *J. Electrochem. Soc.* **2001**, *148*, A1−A6.
(7) Kitani, A.; Kaya, M.; Sasaki, K. *J. Electrochem. Soc.* **1986**, *133*, 1069−1073.
(8) Ghenaatian, H. R.; Mousavi, M. F.; Rahmanifar, M. S. *Electrochim. Acta* **2012**, *78*, 212−222.
(9) Macdiarmid, A. G.; Yang, L. S.; Huang, W. S.; Humphrey, B. D. *Synth. Met.* **1987**, *18*, 393−398.
(10) Cao, Y.; Smith, P.; Heeger, A. J. *Synth. Met.* **1992**, *48*, 91−97.
(11) Kang, E. T.; Neoh, K. G.; Tan, K. L. *Prog. Polym. Sci.* **1998**, *23*, 277−324.
(12) Huang, J. X.; Kaner, R. B. *Angew. Chem., Int. Ed.* **2004**, *43*, 5817−5821.
(13) Shao, L.; Jeon, J.-W.; Lutkenhaus, J. L. *Chem. Mater.* **2012**, *24*, 181−189.
(14) Jeon, J. W.; Ma, Y. G.; Mike, J. F.; Shao, L.; Balbuena, P. B.; Lutkenhaus, J. L. *Phys. Chem. Chem. Phys.* **2013**, *15*, 9654−9662.
(15) Mike, J. F.; Lutkenhaus, J. L. *ACS Macro Lett.* **2013**, *2*, 839−844.
(16) Yoo, J. E.; Lee, K. S.; Garcia, A.; Tarver, J.; Gomez, E. D.; Baldwin, K.; Sun, Y. M.; Meng, H.; Nguyen, T. Q.; Loo, Y. L. *Proc. Natl. Acad. Sci. U.S.A.* **2010**, *107*, 5712−5717.
(17) Tarver, J.; Yoo, J. E.; Loo, Y. L. *Chem. Mater.* **2010**, *22*, 2333−2340.
(18) Heller, A.; Feldman, B. J.; Mano, N.; Loo, Y.-L. Crosslinked adduct of polyaniline an dpolymer acid containing redox enzyme for electrochemical sensor. Abbott Diabetes Care Inc.: 2011.
(19) Yoo, J. E.; Bucholz, T. L.; Jung, S. Y.; Loo, Y. L. *J. Mater. Chem.* **2008**, *18*, 3129−3135.
(20) Lutkenhaus, J. L.; Hammond, P. T. *Soft Matter* **2007**, *3*, 804−816.
(21) Decher, G. *Science* **1997**, *277*, 1232−1237.
(22) Vidyasagar, A.; Sung, C.; Gamble, R.; Lutkenhaus, J. L. *ACS Nano* **2012**, *6*, 6174−6184.
(23) Tang, Z. Y.; Wang, Y.; Podsiadlo, P.; Kotov, N. A. *Adv. Mater.* **2006**, *18*, 3203−3224.
(24) Ariga, K.; Hill, J. P.; Ji, Q. M. *Phys. Chem. Chem. Phys.* **2007**, *9*, 2319−2340.
(25) Cho, J.; Char, K.; Hong, J. D.; Lee, K. B. *Adv. Mater.* **2001**, *13*, 1076.
(26) Schlenoff, J. B.; Dubas, S. T.; Farhat, T. *Langmuir* **2000**, *16*, 9968−9969.
(27) Kim, S. Y.; Hong, J.; Kavian, R.; Lee, S. W.; Hyder, M. N.; Shao-Horn, Y.; Hammond, P. T. *Energy Environ. Sci.* **2013**, *6*, 888−897.
(28) Hyder, M. N.; Lee, S. W.; Cebeci, F. Ç.; Schmidt, D. J.; Shao-Horn, Y.; Hammond, P. T. *ACS Nano* **2011**, *5*, 8552−8561.
(29) DeLongchamp, D. M.; Kastantin, M.; Hammond, P. T. *Chem. Mater.* **2003**, *15*, 1575−1586.
(30) DeLongchamp, D.; Hammond, P. T. *Adv. Mater.* **2001**, *13*, 1455.
(31) Yoo, J. E.; Cross, J. L.; Bucholz, T. L.; Lee, K. S.; Espe, M. P.; Loo, Y. L. *J. Mater. Chem.* **2007**, *17*, 1268−1275.
(32) Cheung, J. H.; Stockton, W. B.; Rubner, M. F. *Macromolecules* **1997**, *30*, 2712−2716.
(33) Wang, Y.; Qian, W. P.; Tan, Y.; Ding, S. H.; Zhang, H. Q. *Talanta* **2007**, *72*, 1134−1140.
(34) Sung, C.; Vidyasagar, A.; Hearn, K.; Lutkenhaus, J. L. *Langmuir* **2012**, *28*, 8100−8109.
(35) Gu, X. K.; Knorr, D. B.; Wang, G. J.; Overney, R. M. *Thin Solid Films* **2011**, *519*, 5955−5961.
(36) Laufer, G.; Kirkland, C.; Cain, A. A.; Grunlan, J. C. *ACS Appl. Mater. Interfaces* **2012**, *4*, 1643−1649.
(37) Yang, Y. H.; Haile, M.; Park, Y. T.; Malek, F. A.; Grunlan, J. C. *Macromolecules* **2011**, *44*, 1450−1459.
(38) Lee, D.; Omolade, D.; Cohen, R. E.; Rubner, M. F. *Chem. Mater.* **2007**, *19*, 1427−1433.
(39) Zakharova, L. Y.; Ibragimova, A. R.; Valeeva, F. G.; Zakharov, A. V.; Mustafina, A. R.; Kudryavtseva, L. A.; Harlampidi, H. E.; Konovalov, A. I. *Langmuir* **2007**, *23*, 3214−3224.

(40) Tarachiwin, L.; Kiattibutr, P.; Ruangchuay, L.; Sirivat, A.; Schwank, J. *Synth. Met.* **2002**, *129*, 303−308.
(41) Chen, R.; Benicewicz, B. C. *Synth. Met.* **2004**, *146*, 133−137.
(42) Huang, W. S.; Macdiarmid, A. G. *Polymer* **1993**, *34*, 1833−1845.
(43) Tarver, J.; Yoo, J. E.; Dennes, T. J.; Schwartz, J.; Loo, Y. L. *Chem. Mater.* **2009**, *21*, 280−286.
(44) Murthy, A.; Manthiram, A. *Chem. Commun.* **2011**, *47*, 6882−6884.
(45) Vaschetto, M. E.; Retamal, B. A. *J. Phys. Chem. A* **1997**, *101*, 6945−6950.
(46) Xia, Y. N.; Wiesinger, J. M.; Macdiarmid, A. G.; Epstein, A. J. *Chem. Mater.* **1995**, *7*, 443−445.
(47) Macdiarmid, A. G.; Epstein, A. J. *Synth. Met.* **1994**, *65*, 103−116.
(48) Ping, Z. *J. Chem. Soc., Faraday Trans.* **1996**, *92*, 3063−3067.
(49) Baibarac, M.; Baltog, I.; Lefrant, S.; Mevellec, J. Y.; Chauvet, O. *Chem. Mater.* **2003**, *15*, 4149−4156.
(50) Murugan, A. V.; Muraliganth, T.; Manthiram, A. *Chem. Mater.* **2009**, *21*, 5004−5006.
(51) Sun, Y.; Macdiarmid, A. G.; Epstein, A. J. *J. Chem. Soc., Chem. Commun.* **1990**, 529−531.
(52) Silverstein, R. M.; Webster, F. X. *Spectrometric identification of organic compounds*, 6th ed.; John Wiley & Sons, Inc.: New York, 1998.
(53) Li, J.; Zhu, L. H.; Wu, Y. H.; Harima, Y.; Zhang, A. Q.; Tang, H. Q. *Polymer* **2006**, *47*, 7361−7367.
(54) Hao, Q. L.; Wang, H. L.; Yang, X. J.; Lu, L. D.; Wang, X. *Nano Res.* **2011**, *4*, 323−333.
(55) Morita, M.; Miyazaki, S.; Tanoue, H.; Ishikawa, M.; Matsuda, Y. *J. Electrochem. Soc.* **1994**, *141*, 1409−1413.
(56) Morita, M.; Miyazaki, S.; Ishikawa, M.; Matsuda, Y.; Tajima, H.; Adachi, K.; Anan, F. *J. Power Sources* **1995**, *54*, 214−217.
(57) Osaka, T.; Momma, T.; Nishimura, K. *Chem. Lett.* **1992**, 1787−1790.
(58) Liu, L.; Tian, F. H.; Zhou, M.; Guo, H. P.; Wang, X. Y. *Electrochim. Acta* **2012**, *70*, 360−364.
(59) Heinze, J.; Dietrich, M.; Mortensen, J. *Macromol. Symp.* **1987**, *8*, 73−81.
(60) Cutler, C. A.; Bouguettaya, M.; Reynolds, J. R. *Adv. Mater.* **2002**, *14*, 684−688.
(61) D'Aprano, G.; Leclerc, M.; Zotti, G. *Macromolecules* **1992**, *25*, 2145−2150.
(62) Bazito, F. F. C.; Silveira, L. T.; Torresi, R. M.; de Torresi, S. I. C. *Phys. Chem. Chem. Phys.* **2008**, *10*, 1457−1462.